

# New approaches to MRS of Cerebral Disorders

Stefan Blüml, Ph.D.

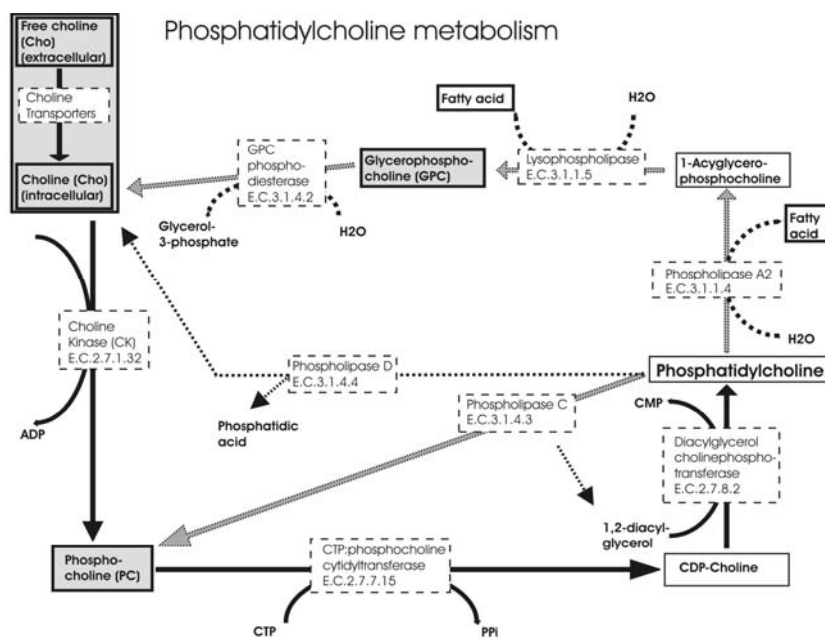
Childrens Hospital Los Angeles, Department of Radiology  
USC Keck School of Medicine

## Phosphorous MR spectroscopy

In the early days of MRS it was believed that  $^{31}\text{P}$  MRS would emerge as the most useful *in vivo* method. The reason was that with  $^{31}\text{P}$  MRS **ATP**, the most widely distributed high-energy compound within the human body - used for all energy requiring processes -, inorganic phosphate (**Pi**), and phosphocreatine (**PCr**) can be observed *in vivo*. Apart from studying energy metabolism,  $^{31}\text{P}$  MRS can also detect phosphorylated metabolites of membrane lipids and can thus be used to study diseases of abnormal membrane metabolism. Phosphorous MRS is by no means a new approach. Indeed a significant number cerebral disorders were studied with  $^{31}\text{P}$  MRS (1-19). However, the emergence of MR imaging as the probably most powerful diagnostic imaging modality and the availability of more sensitive proton spectroscopy diminished the role of  $^{31}\text{P}$  MRS in basic and clinical research. Still, this has not changed the fact that  $^{31}\text{P}$  MRS provides unique information about the status of tissue.  $^{31}\text{P}$  MRS is particularly promising when **proton decoupling**, until now only infrequently utilized, is applied. It is therefore predicted - also because the arrival of more powerful 3T magnets offers the much needed improved sensitivity - that  $^{31}\text{P}$  will re-emerge as an important tool to study cerebral disorders *in vivo*.

## Application: Choline metabolism of tumors

Choline containing metabolites are involved in synthesis and breakdown of phosphatidylcholine, an important membrane phospholipid (**Fig. 1**). Altered levels of choline have been consistently observed in human brain tumors. Indeed, abnormal choline metabolism appears to be a common feature for most forms of cancer including cell lines, animal models of cancer, and various tumors of humans studied *in vivo* (20,21). In particular elevated intracellular phosphocholine (**PC**) pools are associated with increased malignancy.



Adapted from Glunde et al. Cancer Res 2004;64(12):4270-4276.

**FIG. 1:** Choline containing metabolites are involved in synthesis and breakdown of phosphatidylcholine an important membrane phospholipid.  $^1\text{H}$  MRS can be used to measure the sum of all choline containing compounds. PC and GPC can be observed with proton-decoupled  $^{31}\text{P}$  MRS.

With  $^1\text{H}$  MRS only the total choline, which comprises PC, glycerophosphocholine (GPC), free choline (fCho), and possibly other choline containing metabolites, can be quantified. For a more detailed study of choline metabolism the contribution of PC and GPC to the total choline peak needs to be determined. This is best accomplished with  $^{31}\text{P}$  MRS. A problem of standard  $^{31}\text{P}$  MRS at clinical field strength is that PC and phosphoethanolamine (PE) and GPC and glycerophosphoethanolamine (GPE) are partially overlapping due to hetero-nuclear J-couplings with protons. **Proton decoupling** is required to collapse the PC, PE, GPC, GPE multiplets into single peaks (22) (**Fig. 2**).

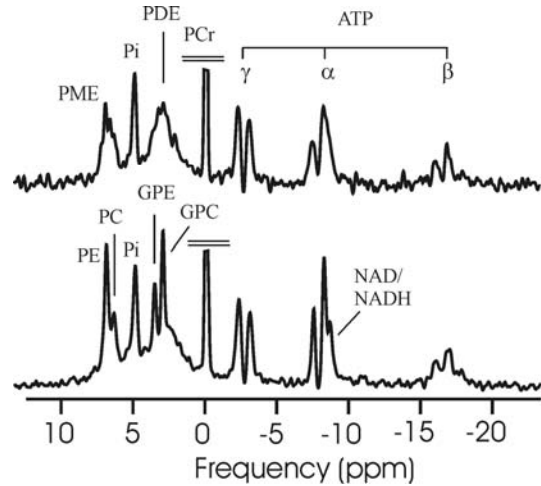


**FIG. 2:**  $^{31}\text{P}$  (upper trace) and proton decoupled  $^{31}\text{P}$  spectra of (normal) brain tissue. PCr peaks are truncated.

### Pediatric brain tumors

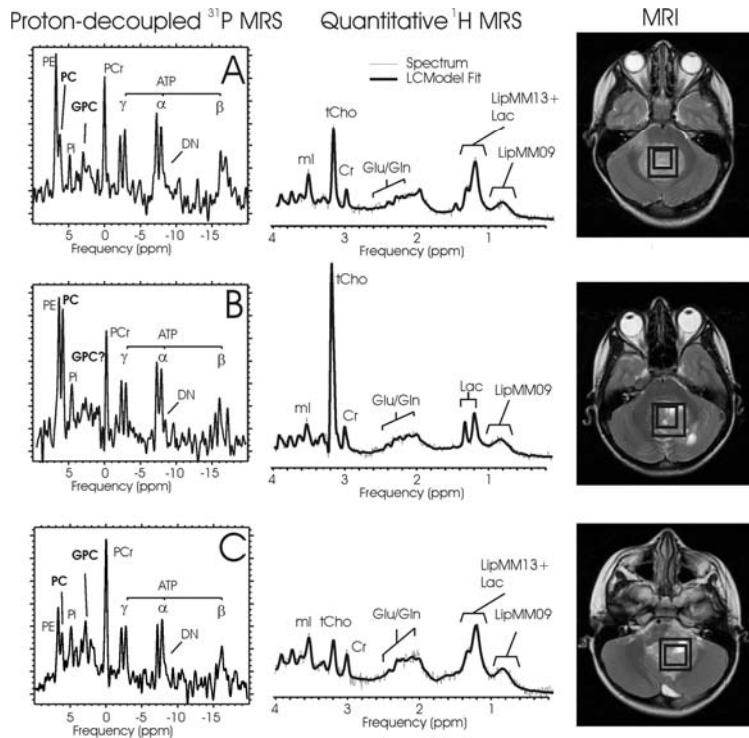


**FIG. 3:** Proton-decoupled  $^{31}\text{P}$  MRS,  $^1\text{H}$  MRS, and MRI of cerebellar medulloblastoma (A+B) and, anaplastic ependymoma (C).  $^{31}\text{P}$  spectra are scaled to ATP as an internal reference.  $^1\text{H}$  spectra are scaled to measured absolute concentrations to allow direct comparison with each other. Areas or amplitudes of  $^{31}\text{P}$  and  $^1\text{H}$  spectra can not be directly compared. All spectra were acquired on a clinical 1.5 T scanner. A custom-designed dual tuned head coil was used for clinically indicated MR imaging, proton MRS, and for experimental  $^{31}\text{P}$  MRS. The total examination time was approximately 70 min and  $^1\text{H}$  and  $^{31}\text{P}$  acquisitions were integrated in routine pre-operative work-up of patients. ROIs for  $^1\text{H}$  (small box) and  $^{31}\text{P}$  are marked on MRI, respectively.

$^1\text{H}$  and  $^{31}\text{P}$  spectra and MR images of pediatric patients with **untreated brain tumors** are shown in **Fig. 3**. Proton spectra were acquired with a single voxel PRESS sequence (TE = 35ms). A slice selective spinecho sequence with 2D phase encoding was used for  $^{31}\text{P}$  MRS. Aggressive medulloblastoma have prominent peaks from PE and PC, whereas GPE and GPC are difficult to discern from the noise signal. Significant variations of the metabolic profile in individual tumors of the same pathological type were noted. This is illustrated in the two cases of medulloblastoma shown in **Fig. 3A,B** where PC levels were strikingly different. A high PC/GPC ratio has been

postulated to be a marker for more malignant tumors. To what extent the measurements of PC and GPC (and total choline with  $^1\text{H}$  MRS) are of predictive value in individual patients and can be used for patient stratification needs to be determined by long-term follow-up. A comparison of  $^1\text{H}$  and  $^{31}\text{P}$  spectra also reveals that a significant fraction of choline in tumors is not accounted for by PC+GPC. This is in contrast to normal brain where total choline  $\approx$  1/3 PC+ 2/3 GPC (13,15).

### **Carbon spectroscopy**

The low natural abundance of  $^{13}\text{C}$  (1.1%) and its inherent low sensitivity (1/50 of hydrogen) render *in vivo*  $^{13}\text{C}$  MRS studies in humans very challenging. However, with the infusion of  $^{13}\text{C}$  labeled substrates, such as glucose or acetate, highly specific information about metabolites and metabolic rates can be obtained (23-27). In a typical experiment, e.g. intravenously or orally administered  $^{13}\text{C}$  labeled glucose, enters the blood stream, passes the blood-brain-barrier, and is detected within 1-2 minutes after administration in  $^{13}\text{C}$  spectra. Subsequently glucose is broken down through glycolysis and oxidation in the tricarboxylic acid (TCA)-cycle.  $^{13}\text{C}$  label accumulation can then be detected in all metabolites of sufficient high concentration involved in glucose oxidation. From the time courses of label accumulation important flux rates such as the TCA-cycle activity and glutamine synthesis have been determined. For a more detailed update on methods and progress in  $^{13}\text{C}$  MRS the reader is referred to a recent issue of *NMR in Biomedicine* (28) exclusively dedicated to the application of  $^{13}\text{C}$  MRS to study biological systems and references therein.

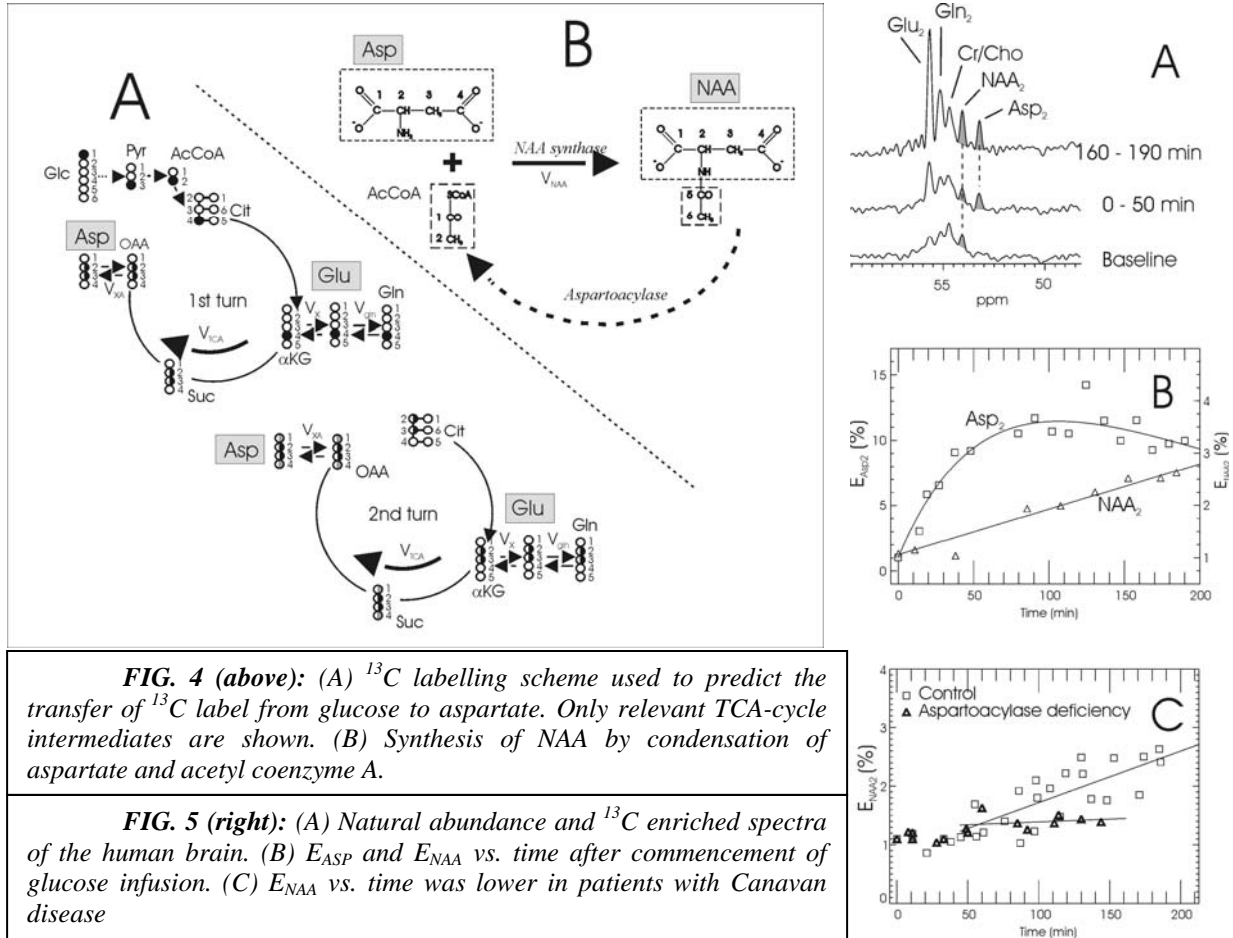
As for  $^{31}\text{P}$  MRS, special hardware is required for  $^{13}\text{C}$  MRS. Presently, even for “niche” manufacturers,  $^{13}\text{C}$  RF coils are too “exotic” and most groups conducting *in vivo*  $^{13}\text{C}$  research have built their own coils. Volume coils are more flexible and have a special advantage when quantitation of cerebral metabolites is the goal. Nevertheless, surface coils have exclusively been used for  $^{13}\text{C}$  MRS since they provide the much-needed extra signal required for *in vivo*  $^{13}\text{C}$  MRS. Because all  $^{13}\text{C}$  methods either apply direct detection with proton-decoupling, polarization transfer, or hetero-nuclear editing, dual-tuned coils ( $^1\text{H}$  and  $^{13}\text{C}$  frequencies) are required. Because of the technical and logistical challenges and the need for large amounts of  $^{13}\text{C}$  labeled substrates (expensive) it is not surprising that there have been only a few patient studies. As of now, *in vivo*  $^{13}\text{C}$  MRS may be more appropriate for studies of small groups of patients. This may change with more support from manufactures towards the implementation of  $^{13}\text{C}$  MRS on clinical systems, a drop of the price of  $^{13}\text{C}$  labeled compounds, and the development of efficient infusion protocols. For some applications oral administration may be appropriate (27,29,30) which would simplify the procedure considerably because one inter-venous (i.v.) infusion line could be eliminated.

### **Application: Direct determination of the NAA-synthesis rate *in vivo* by $^{13}\text{C}$ MRS after 1- $^{13}\text{C}$ glucose infusion**

To illustrate the potential of  $^{13}\text{C}$  MRS to address specific biological questions the determination of the N-acetyl-aspartate (NAA) synthesis rate ( $V_{\text{NAA}}$ ) *in vivo* in human brain is illustrated (27). NAA is an amino acid derivative in vertebrate brain that reaches its highest concentrations in neurons and axons. It is principally synthesized in neurons by energy dependent condensation of aspartate and acetyl coenzyme A, catalysed by the mitochondrial enzyme NAA synthase, and is then exported to the cytosolic compartment. The enzyme to breakdown NAA (N-aspartoacylase, E.C. 35.1.15) is located in oligodendrocytes. Therefore, NAA apparently cycles between neuronal and glial compartments. The role of NAA, and its

regulation *in vivo*, is not well understood (31,32). Hypothetically, disorders of synthesis or breakdown of NAA may contribute to altered steady-state concentrations of NAA. To date, only one definitive disorder of NAA metabolism has been identified, Canavan disease, where N-aspartoacylase deficiency causes increased cerebral NAA concentrations.

For the determination of  $V_{NAA}$ , 1- $^{13}C$  glucose was infused and direct detected  $^{13}C$  MRS with proton decoupling was utilized. As illustrated in **Fig. 4A**, the  $^{13}C$  label from glucose enters the TCA-cycle at citrate and enriches glutamate C<sub>4</sub>, succinate C<sub>2,3</sub> (Suc) and oxaloacetate C<sub>2,3</sub> (OAA) during the first turn. From OAA,  $^{13}C$  label is transferred to aspartate and then on to NAA (**Fig. 4B**).



It is assumed that under steady-state NAA is synthesized from aspartate and catabolized at the same rate. The NAA synthesis rate ( $V_{NAA}$ ) can then be determined from the measured time courses of  $^{13}C$  accumulation in aspartate and NAA (**Fig. 5**) by iteratively resolving the differential equation:

$$d/dt [NAA^*] = E_{Asp}V_{NAA} - E_{NAA}V_{NAA} \text{ (Fig. 6).}$$

- $E_{NAA}$  fractional  $^{13}C$  enrichment of NAA
- $[NAA^*]$  concentration of  $^{13}C$  enriched NAA
- $E_{Asp}$  fractional  $^{13}C$  enrichment of aspartate

The NAA synthesis rate obtained in controls ( $9 \pm 4$  nmol/g/min) with this method is consistent with data obtained from cortex of rat (33-35). The turnover time of NAA from aspartate in controls is approximately 19 hours ( $[NAA] \approx 10$  mmol/kg in controls - determined with  $^1\text{H}$  MRS). In Canavan disease a significant lower rate of NAA synthesis ( $4 \pm 0$  nmol/g/min) was observed which is consistent with what has been estimated from urine excretion of NAA in this disease (36-38). Note,

in the absence of breakdown of NAA in the brain, excretion through urine is the main pathway for NAA to leave the system. The turnover time in Canavan disease is approximately 60 h ( $[NAA] \approx 15$  mmol/kg in Canavan disease). An explanation for the reduced NAA synthesis rate in Canavan disease could be feedback inhibition.

## Summary

As illustrated above with two examples, multinuclear spectroscopy can add important information about metabolism of diseased brain. For researchers to take advantage of the potential of  $^{31}\text{P}$  and  $^{13}\text{C}$  MRS to study brain diseases, these modalities need to be integrated on clinical MR systems. Once accomplished, a unique portfolio of methods, MRI, fMRI, DTI, etc, and multinuclear MRS, is available to the clinical and basic researchers. The value of each modality will be amplified and new avenues to study cerebral disorders will be opened.

## References

1. Cady EB, Costello AM, Dawson MJ, Delpy DT, Hope PL, Reynolds EO, Tofts PS, Wilkie DR. Non-invasive investigation of cerebral metabolism in newborn infants by phosphorus nuclear magnetic resonance spectroscopy. *Lancet* 1983;1(8333):1059-1062.
2. Azzopardi D, Wyatt JS, Cady EB, Delpy DT, Baudin J, Stewart AL, Hope PL, Hamilton PA, Reynolds EO. Prognosis of newborn infants with hypoxic-ischemic brain injury assessed by phosphorus magnetic resonance spectroscopy. *Pediatr Res* 1989;25(5):445-451.
3. Calabrese G, Deicken RF, Fein G, Merrin EL, Schoenfeld F, Weiner MW.  $^{31}\text{P}$  magnetic resonance spectroscopy of the temporal lobes in schizophrenia. *Biol Psychiatry* 1992;32(1):26-32.
4. Laxer KD, Huesch B, Sappey-Marini D, Weiner MW. Increased pH and inorganic phosphate in temporal seizure foci demonstrated by  $^{31}\text{P}$  MRS. *Epilepsia* 1992;33(4):618-623.
5. Hugg JW, Duijn JH, Matson GB, Maudsley AA, Tsuruda JS, Gelinas DF, Weiner MW. Elevated lactate and alkalosis in chronic human brain infarction observed by  $^1\text{H}$  and  $^{31}\text{P}$  MR spectroscopic imaging. *J Cereb Blood Flow Metab* 1992;12(5):734-744.

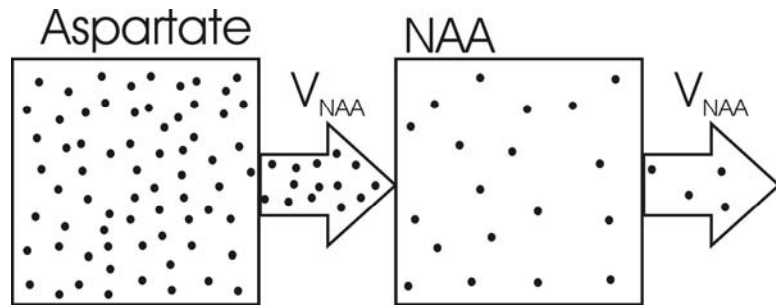


**FIG. 6:** At steady-state the total number of synthesized and catabolised NAA molecules is equal. However, the number of  $^{13}\text{C}$  labeled NAA molecules synthesized (per time unit) is given by the fractional enrichment of the precursor Asp ( $E_{\text{Asp}}$ ) times the total flux. The number of NAA molecules broken down (per time unit) is given by the fractional enrichment of NAA ( $E_{\text{NAA}}$ ) times the total flux. There is no further net increase of  $^{13}\text{C}$  labeled NAA once the fractional enrichment of the Asp and NAA pools are equal.

6. Younkin DP, Delivoria-Papadopoulos M, Maris J, Donlon E, Clancy R, Chance B. Cerebral metabolic effects of neonatal seizures measured with in vivo <sup>31</sup>P NMR spectroscopy. *Ann Neurol* 1986;20(4):513-519.
7. Husted CA, Goodin DS, Hugg JW, Maudsley AA, Tsuruda JS, de Bie SH, Fein G, Matson GB, Weiner MW. Biochemical alterations in multiple sclerosis lesions and normal-appearing white matter detected by in vivo <sup>31</sup>P and <sup>1</sup>H spectroscopic imaging. *Ann Neurol* 1994;36(2):157-165.
8. Deicken RF, Calabrese G, Merrin EL, Meyerhoff DJ, Dillon WP, Weiner MW, Fein G. <sup>31</sup>phosphorus magnetic resonance spectroscopy of the frontal and parietal lobes in chronic schizophrenia. *Biol Psychiatry* 1994;36(8):503-510.
9. Pettegrew JW, Keshavan MS, Minshew NJ. <sup>31</sup>P nuclear magnetic resonance spectroscopy: neurodevelopment and schizophrenia. *Schizophr Bull* 1993;19(1):35-53.
10. Bluml S, Tan J, Harris K, Adatia N, Karne A, Sproull T, Ross B. Quantitative proton-decoupled <sup>31</sup>P MRS of the schizophrenic brain in vivo. *J Comput Assist Tomogr* 1999;23(2):272-275.
11. Barbiroli B, Montagna P, Martinelli P, Lodi R, Iotti S, Cortelli P, Funicello R, Zaniol P. Defective brain energy metabolism shown by in vivo <sup>31</sup>P MR spectroscopy in 28 patients with mitochondrial cytopathies. *J Cereb Blood Flow Metab* 1993;13(3):469-474.
12. Gonzalez RG, Guimaraes AR, Moore GJ, Crawley A, Cupples LA, Growdon JH. Quantitative in vivo <sup>31</sup>P magnetic resonance spectroscopy of Alzheimer disease. *Alzheimer Dis Assoc Disord* 1996;10(1):46-52.
13. Albers MJ, Krieger MD, Gonzalez-Gomez I, Gilles FH, McComb JG, Nelson MD, Jr., Bluml S. Proton-decoupled (<sup>31</sup>)P MRS in untreated pediatric brain tumors. *Magn Reson Med* 2005;53(1):22-29.
14. Bluml S, Philippart M, Schiffmann R, Seymour K, Ross BD. Membrane Phospholipids and High-Energy Metabolites in Childhood Ataxia with CNS Hypomyelination. *Neurology* 2003;61:648-654.
15. Bluml S, Seymour KJ, Ross BD. Developmental changes in choline- and ethanolamine-containing compounds measured with proton-decoupled (<sup>31</sup>)P MRS in in vivo human brain. *Magn Reson Med* 1999;42(4):643-654.
16. Bluml S, Zuckerman E, Tan J, Ross BD. Proton-decoupled <sup>31</sup>P magnetic resonance spectroscopy reveals osmotic and metabolic disturbances in human hepatic encephalopathy. *Journal of Neurochemistry* 1998;71(4):1564-1576.
17. Hoang TQ, Bluml S, Dubowitz DJ, Moats R, Kopyov O, Jacques D, Ross BD. Quantitative proton-decoupled <sup>31</sup>P MRS and <sup>1</sup>H MRS in the evaluation of Huntington's and Parkinson's diseases. *Neurology* 1998;50(4):1033-1040.
18. Tan J, Bluml S, Hoang T, Dubowitz D, Mevenkamp G, Ross B. Lack of effect of oral choline supplement on the concentrations of choline metabolites in human brain. *Magnetic Resonance in Medicine* 1998;39(6):1005-1010.
19. Negendank W, Li CW, Padavic-Shaller K, Murphy-Boesch J, Brown TR. Phospholipid metabolites in <sup>1</sup>H-decoupled <sup>31</sup>P MRS in vivo in human cancer: implications for experimental models and clinical studies. *Anticancer Res* 1996;16(3B):1539-1544.
20. Ackerstaff E, Glunde K, Bhujwala ZM. Choline phospholipid metabolism: a target in cancer cells? *J Cell Biochem* 2003;90(3):525-533.
21. Podo F. Tumour phospholipid metabolism. *NMR Biomed* 1999;12(7):413-439.

22. Luyten PR, Bruntink G, Sloff FM, Vermeulen JW, van der Heijden JI, den Hollander JA, Heerschap A. Broadband proton decoupling in human  $^{31}\text{P}$  NMR spectroscopy. *NMR Biomed* 1989;1(4):177-183.
23. Mason GF, Gruetter R, Rothman DL, Behar KL, Shulman RG, Novotny EJ. Simultaneous determination of the rates of the TCA cycle, glucose utilization, alpha-ketoglutarate/glutamate exchange, and glutamine synthesis in human brain by NMR. *J Cereb Blood Flow Metab* 1995;15(1):12-25.
24. Gruetter R, Novotny EJ, Boulware SD, Mason GF, Rothman DL, Shulman GI, Prichard JW, Shulman RG. Localized  $^{13}\text{C}$  NMR spectroscopy in the human brain of amino acid labeling from D-[1- $^{13}\text{C}$ ]glucose. *Journal of Neurochemistry* 1994;63(4):1377-1385.
25. Bluml S, Moreno-Torres A, Shic F, Nguy CH, Ross BD. Tricarboxylic acid cycle of glia in the in vivo human brain. *NMR Biomed* 2002;15(1):1-5.
26. Lebon V, Petersen KF, Cline GW, Shen J, Mason GF, Dufour S, Behar KL, Shulman GI, Rothman DL. Astroglial contribution to brain energy metabolism in humans revealed by  $^{13}\text{C}$  nuclear magnetic resonance spectroscopy: elucidation of the dominant pathway for neurotransmitter glutamate repletion and measurement of astrocytic oxidative metabolism. *J Neurosci* 2002;22(5):1523-1531.
27. Moreno A, Ross BD, Bluml S. Direct determination of the N-acetyl-L-aspartate synthesis rate in the human brain by ( $^{13}\text{C}$ ) MRS and [1-( $^{13}\text{C}$ )]glucose infusion. *J Neurochem* 2001;77(1):347-350.
28. *NMR Biomed* 2003;16(6-7):301-457.
29. Moreno A, Bluml S, Hwang JH, Ross BD. Alternative 1-( $^{13}\text{C}$ ) glucose infusion protocols for clinical ( $^{13}\text{C}$ ) MRS examinations of the brain. *Magnetic Resonance in Medicine* 2001;46(1):39-48.
30. Watanabe H, Umeda M, Ishihara Y, Okamoto K, Oshio K, Kanamatsu T, Tsukada Y. Human brain glucose metabolism mapping using multislice 2D (1)H-( $^{13}\text{C}$ ) correlation HSQC spectroscopy. *Magnetic Resonance in Medicine* 2000;43(4):525-533.
31. Tallan HH. Studies on the distribution of N-acetyl-L-aspartic acid in brain. *J Biol Chem* 1957;224(1):41-45.
32. Baslow MH. Functions of N-acetyl-L-aspartate and N-acetyl-L-aspartylglutamate in the vertebrate brain: role in glial cell-specific signaling. *Journal of Neurochemistry* 2000;75(2):453-459.
33. Truckenmiller ME, Namboodiri MA, Brownstein MJ, Neale JH. N-Acetylation of L-aspartate in the nervous system: differential distribution of a specific enzyme. *Journal of Neurochemistry* 1985;45(5):1658-1662.
34. Burri R, Steffen C, Herschkowitz N. N-acetyl-L-aspartate is a major source of acetyl groups for lipid synthesis during rat brain development. *Developmental Neuroscience* 1991;13(6):403-411.
35. Choi IY, Gruetter R. Dynamic or inert metabolism? Turnover of N-acetyl aspartate and glutathione from D-[1- $^{13}\text{C}$ ]glucose in the rat brain in vivo. *J Neurochem* 2004;91(4):778-787.
36. Kvittingen EA, Guibaud PP, Divry P, Mandon G, Rolland MO, Domenichini Y, Jakobs C, Christensen E. Prenatal diagnosis of hereditary tyrosinaemia type I by determination of fumarylacetoacetase in chorionic villus material. *Eur J Pediatr* 1986;144(6):597-598.

37. Matalon R, Michals K, Sebesta D, Deanching M, Gashkoff P, Casanova J. Aspartoacylase deficiency and N-acetylaspartic aciduria in patients with Canavan disease. *Am J Med Genet* 1988;29(2):463-471.
38. Burns SP, Chalmers RA, West RJ, Iles RA. Measurement of human brain aspartate N-acetyl transferase flux in vivo. *Biochem Soc Trans* 1992;20(2):107S.